

Quantum Lyapunov control with machine learning

S. C. Hou and X. X. Yi*

*Center for Quantum Sciences and School of Physics,
Northeast Normal University, Changchun 130024, China*

(Dated: August 9, 2018)

Quantum state engineering is a central task in Lyapunov-based quantum control. Given different initial states, better performance may be achieved if the control parameters, such as the Lyapunov function, are individually optimized for each initial state, however, at the expense of computing resources. To tackle this issue, we propose an initial-state-adaptive Lyapunov control strategy with machine learning, specifically, artificial neural networks trained through supervised learning. Two designs are presented and illustrated where the feedforward neural network and the general regression neural network are used to select control schemes and design Lyapunov functions, respectively. Since the sample generation and the training of neural networks are carried out in advance, the initial-state-adaptive Lyapunov control can be implemented without much increase of computational resources.

I. INTRODUCTION

Quantum control [1, 2] plays a fundamental role in modern quantum technologies such as quantum computation, quantum communication and quantum metrology. A central goal in quantum control is designing time-varying external control fields to effectively engineer quantum states and operators. More than a decade ago, the Lyapunov-based method was developed for the control of quantum systems [3, 4]. In quantum Lyapunov control, the control fields are obtained by simulating the dynamics (in feedback form) only once and then applied in an open-loop scenario. The method has the merits of simplicity in generating control fields and flexibility in designing the control field shapes. In recent years, numerous efforts have been devoted to investigate or improve the convergence of Lyapunov control for different quantum control models [5–12]. Meanwhile, Lyapunov control method is successfully employed for diverse quantum information processing tasks [12–23]. For example, it is recently used to realize topological modes [19], quantum synchronization [21] and speed up adiabatic passage [22].

In previous research, the designs of quantum Lyapunov control are usually initial-state-independent. When dealing with different initial states, better performance (e.g. control time or fidelity) may be achieved if the control parameters (such as those in the Lyapunov function) are individually optimized for each initial state. However, it is usually hard to find an explicit (analytic) relationship between the optimal control parameters and the initial states since the control fields are generated numerically. On the other hand, numerical optimizing the Lyapunov control parameters typically requires simulating the dynamics more than once, making quantum Lyapunov control complicated. Thus an initial-state-adaptive quantum Lyapunov control without a significant increase of com-

puting resources is desirable.

Machine learning [24, 25] is a powerful tool to improve a performance criterion from experience or data, which has been extensively applied in internet technology, artificial intelligence, finance, medical diagnosis and so on. Recently, machine learning technology has been successfully employed to advance quantum physics problems [26–36], such as quantum many-body problems [30, 31], quantum state identification [31, 32] and quantum control [33–36]. Motivated by its ability and versatility, we intend to use machine learning techniques, specifically, (artificial) neural networks [25] to design an initial-state-adaptive quantum Lyapunov control. The basic idea is as follows. First, numerically generate a certain number of samples that encode different initial states and their corresponding optimal parameters. Then, train a neural network with these samples through supervised learning until its performance is satisfactory. At last, apply the trained neural network to predict control parameters for new initial states. Two designs are proposed to select control schemes and design Lyapunov functions. The initial-state-adaptive designs would be helpful when the number of initial states is large or real-time control is needed.

The remainder of the paper is organized as follows. Sec.II reviews the Lyapunov control method for the eigenstate preparation problem. In Sec.III, we introduce the feedforward neural network (multilayer perceptron) and the general regress neural network (GRNN) which are used as the tools for classification and regression in this paper, respectively. The two initial-state-adaptive designs are proposed in Sec.IV and then illustrated with a three-level quantum system in Sec.V. Finally, the results are summarized and discussed in Sec.VI.

II. QUANTUM LYAPUNOV CONTROL

Quantum Lyapunov control is a useful technique for quantum control tasks, typically eigenstate control [13, 15, 16, 18, 20, 22, 23]. It consists of two steps. In the first

*Electronic address: yixx@nenu.edu.cn

step, time-dependent control fields are numerically calculated by simply one simulation of the system dynamics (in feedback form). In the second step, the generated control fields are used in applications (experiments) in an open-loop way.

We introduce the mathematical formula of quantum Lyapunov control with a n -dimensional closed quantum system described by the Schrödinger equation ($\hbar = 1$ is assumed)

$$\frac{d}{dt}|\Psi\rangle = -i[H_0 + \sum_{k=1}^m f_k(t)H_k]|\Psi\rangle. \quad (1)$$

Here H_0 is the system (drift) Hamiltonian, H_k is the k th control Hamiltonians and $f_k(t)$ is its corresponding control field which is a time-dependent real function. The aim is to find proper $f_k(t)$ such that the initial state $|\Psi\rangle$ evolves to a desired state $|\Psi_d\rangle$ at some point of time.

In quantum Lyapunov control, a real function V called Lyapunov function (conventionally $V \geq 0$) is assigned and $f(t)$ are designed to guarantee $\dot{V} \leq 0$. Through this, the quantum system is driven to states satisfying $\dot{V} = 0$ as $t \rightarrow \infty$, meanwhile, the desired state is asymptotically reached. The convergence behavior could be analyzed by the La Salle's invariance principle [1]. The choice of Lyapunov function V is not unique. For example, V could be chosen as the distance between the quantum state and the desired state, the expectation value of a Hermitian operator and so on [6]. Here we consider the second form of Lyapunov function, i.e.,

$$V = \langle \psi | P | \psi \rangle, \quad (2)$$

where P is a Hermitian and positive semi-definite operator such that $V \geq 0$. This form is representative and covers some other forms of Lyapunov function such as that based on the Hilbert-Schmidt distance [1]. More importantly, there is freedom in designing P enabling us to optimize it for different initial states for the purpose of this paper.

The control fields could be designed based on the time derivative of V ,

$$\dot{V} = \langle \Psi | i[H_0 + \sum_{k=1}^m f_k(t)H_k, P] | \Psi \rangle \quad (3)$$

$$= \sum_{k=1}^m f_k(t) \langle \Psi | i[H_k, P] | \Psi \rangle \quad (4)$$

where $[H_0, P] = 0$ is assumed to cancel the drift term. This condition could be realized by constructing the hermitian operator P as

$$P = \sum_{l=1}^n p_l |E_l\rangle \langle E_l|. \quad (5)$$

Here $|E_l\rangle$ is the l th eigenstate of H_0 and p_l are non-negative real numbers. In this work, p_l will be optimized

for different initial states and predicted by trained artificial neural networks.

The control fields $f_k(t)$ is conventionally designed as

$$f_k(t) = -K \langle \Psi | i[H_k, P] | \Psi \rangle \quad (6)$$

where K is a real constant associated with the control strength. Other approaches to design the control fields are also investigated to improve the performance of quantum Lyapunov control [8, 10, 11]. From Eq(6), there is

$$\dot{V} = -K^{-1} \sum_{k=1}^m f_k^2(t) \leq 0, \quad (7)$$

i.e., the Lyapunov function keeps non-increasing with the controlled dynamics. With ideal control parameters (e.g. Lyapunov function, control Hamiltonian, design of control fields), the control law determined by Eq.(2,5,6) will drive any initial state $|\Psi(0)\rangle$ (except that satisfies $\dot{V}(0) = 0$) asymptotically to the eigenstate of H_0 with the minimum eigenvalue as $t \rightarrow \infty$. Meanwhile, V will decrease to its minimum.

Obviously, the performance (e.g., fidelity, control time) of quantum Lyapunov control depends on the control parameters such as Lyapunov function V and control Hamiltonian H_k . Choosing appropriate parameters is therefore of great importance for Lyapunov control problems.

III. ARTIFICIAL NEURAL NETWORKS

In this section, we briefly introduce two neural network models used in this paper, feedforward neural network and general regress neural network. Mathematically, these neural networks could be understood as a function that maps an input real vector X to an output real vector Y .

A. Feedforward Neural Network

Feedforward neural network is the most well known neural network. A schematic diagram of a feedforward neural network is shown in Fig.1. A feedforward neural network consists of a layer of input nodes (by squares in Fig.1), an output layer of neurons (processing units, by circles in Fig.1), and possibly a set of hidden layers of neurons. In feedforward neural networks, signal flows from the input layer to the output layer without feedback loops. A feedforward neural network with one or more hidden layers is called a multilayer perceptron [24, 25]. With enough neurons, a multilayer perceptron is able to approximate any continuous nonlinear function and solve many complicated tasks. In a feedforward neural network, the output y of a single neuron is expressed by

$$y = s\left(\sum_{i=1}^m x_i \omega_i + b\right), \quad (8)$$

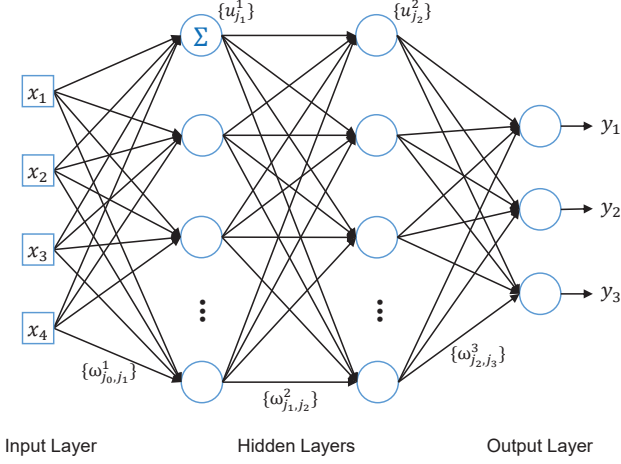


FIG. 1: A schematic diagram of a feedforward neural network with 4 input nodes, 3 hidden layers, and 2 output neurons. Here $j_l = 1, 2, \dots, n_l$ where n_l is the node (neuron) number of the l th layer.

where the x_i is the output of the i th neuron (node) of the last layer, ω_i is the weight of x_i corresponding to the arrows in Fig.1, and b is a bias (threshold) which is omitted in Fig.1. $s(\dots)$ is called an activation function which is usually a nonlinear sigmoid function limiting the strength of the output signal. The logistic function

$$s(x) = \frac{1}{1 + e^{-x}} \quad (9)$$

is used as the activation function in this paper that transfers any input signal to the range 0 to 1.

In a feedforward neural network with m layers of neurons (n_l neurons in the l th layer) and an input layer with n_0 nodes, the input $X = [x_1 \ x_2 \ \dots \ x_{n_0}]^T$ is transformed to the output $Y = [y_1 \ y_2 \ \dots \ y_{n_m}]^T$ by

$$u_{j_1}^1 = s\left(\sum_{j_0=1}^{n_0} x_{j_0} w_{j_0,j_1}^1 + b_{j_1}^1\right), \quad (10)$$

$$u_{j_2}^2 = s\left(\sum_{j_1=1}^{n_1} u_{j_1}^1 w_{j_1,j_2}^2 + b_{j_2}^2\right), \quad (11)$$

\vdots

$$y_{j_m} = s\left(\sum_{j_{m-1}=1}^{n_{m-1}} u_{j_{m-1}}^m w_{j_{m-1},j_m}^m + b_{j_m}^m\right) \quad (12)$$

where $j_l = 1, 2, \dots, n_l$ with $l = 0, 1, \dots, m$. Here $u_{j_l}^\alpha$ is the output of the j_l th neuron of the α th neuron layer. In the above equations, the superscript (1,2,...,m) denotes the index of the neuron layers, and the subscript j_l represents the j_l th neuron or node of the l th layer, as shown in Fig.1. Thus the network is determined by the layer numbers m , node numbers in each layer, weights, biases as well as the activation function.

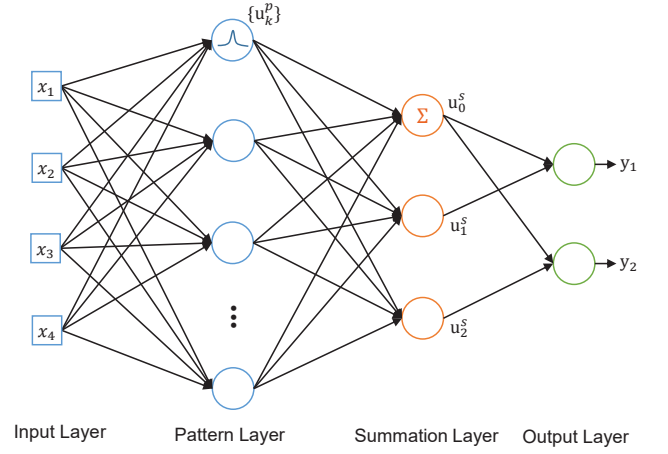


FIG. 2: A schematic diagram of a general regression neural network with 4 input nodes and 2 output neurons.

For a specific problem, the design of the feedforward neuron network structure is generally empirical. The training of a feedforward neuron network is implemented by adjusting its weights and biases. In supervised learning, the weights and biases could be effectively studied by the back-propagation (BP) algorithm [24, 25] with the training samples including a number of input vectors and their target output vectors.

B. General Regression Neural Network

General regression neural network (GRNN) is a type of radial basis function (RBF) network proposed by D. F. Specht in 1991 [37]. It is a powerful tool to estimate continuous variables [38–41] even when the training data is few. A general regression neural network consists of 4 layers: an input layer, a pattern layer, a summation layer and an output layer as shown in Fig.2. In contrast to the feedforward neural network, the neuron number in each layer is fixed in a GRNN and determined from its training samples. For a training set with N samples $\{X^k, Y^k\}, k = 1, 2, \dots, N$ where $X^k = [x_1^k \ x_2^k \ \dots \ x_{n_I}^k]$ is the k th input vector and $Y^k = [y_1^k \ y_2^k \ \dots \ y_{n_O}^k]$ is its target output, the pattern layer neuron number is N , the number of the input (output) layer node is n_I (n_O), and the number of the summation layer neuron is $n_O + 1$.

For an input X , the output of the pattern layer ($u_k^p, k = 1, 2, \dots, N$), the summation layer ($u_{j_s}^s, j_s = 0, 1, 2, \dots, n_O$) and the output layer ($y_j, j = 1, 2, \dots, n_O$)

is given by

$$u_k^p = \exp\left(-\frac{(X - X^k)^T(X - X^k)}{2\sigma^2}\right), \quad (13)$$

$$u_0^s = \sum_{k=1}^N u_k^p, \quad u_{j_s}^s (j_s \neq 0) = \sum_{k=1}^N y_{j_s}^k u_k^p, \quad (14)$$

$$y_j = \frac{u_j^s}{u_0^s}, \quad (15)$$

respectively. The estimation y_j for an input X can be understood as an average of all y_j^k weighted exponentially according to the Euclidean distance between X and X^k . Here σ is called a smoothing parameter ($\sigma > 0$). When σ is small, the estimation y_i for X is closely related to y_i^k whose inputs X^k are close to X . In contrast, when σ is large, y_i approaches the mean of all y_j^k . The GRNN is established as soon as the training samples are stored while the smoothing parameter σ is the only adjustable parameter needed to train.

IV. INITIAL-STATE-ADAPTIVE DESIGNS

When dealing with different initial states, better performances may be achieved if the parameters in quantum Lyapunov control, such as those in the Lyapunov function V or the control Hamiltonian H_k , are optimally chosen for each initial state, i.e., initial-state-adaptive. However, finding optimized parameters typically costs more computing resources (e.g. simulation time) since Lyapunov control fields are calculated numerically. In this way, quantum Lyapunov control would lose its simplicity that the control fields are obtained with only one simulation of system dynamics. To tackle this issue, we propose to design an initial-state-adaptive Lyapunov control with neural networks. As the processes of generating samples and training neural networks are implemented in advance, the computing resources of initial-state-adaptive Lyapunov control with neural networks would not significantly increase in applications. The basic strategy comprises the following steps.

(1) Generate a certain number of initial states whose parameters are randomly distributed in an interested ranges.

(2) Numerically find the optimal control parameters for these initial states. Data from (1) and (2) constitute the training set (testing set if needed).

(3) Build a neural network whose input is associated with the initial state parameters and output associated with the optimal control parameters.

(4) Train the neural network by supervised learning with the training set until the neural network performance is satisfactory.

(5) Apply the trained neural network to predict optimal control parameters for new initial states .

For the eigenstate control problem described in Sec.II,

we propose two designs where the mentioned neural networks are used to select control schemes or predict Lyapunov functions for different initial states. Two important functions of neural networks, classification and regression, are employed.

A. Classification: selecting control schemes

Consider there are several Lyapunov control schemes where the control Hamiltonians, Lyapunov functions or other conditions are different. One of these schemes will be finally adopted in experimental or theoretical application. Our aim is to use neural networks to predict the optimal scheme for each individual initial state.

Specifically, assume there are M candidate control Hamiltonians $H_c (c = 1, 2, \dots, M)$ in which one of them will be selected. Thus the dynamics is described by

$$\frac{d}{dt}|\Psi\rangle = -i[H_0 + f(t)H_c]|\Psi\rangle. \quad (16)$$

Other conditions such as the Lyapunov function V , the strength K , and H_0 are fixed. The task is preparing an eigenstate of H_0 , say, $|E_g\rangle$, as discussed in Sec.II. Given an initial state, we will use a feedforward neural network to predict the control Hamiltonian that leads to the highest fidelity defined by $F = |\langle\Psi(T)|E_g\rangle|^2$ at a certain control time T . The problem is solved by classifying the initial states according to their favorable control Hamiltonian with the feedforward neural network.

For a n -dimensional system, the initial state $|\Psi_0\rangle$ could be parameterized in the eigenbasis of H_0 as

$$\begin{aligned} |\Psi_0\rangle_{n=2} &= \sin\theta_1 e^{i\phi_1}|E_1\rangle + \cos\theta_1|E_2\rangle \\ |\Psi_0\rangle_{n=3} &= \sin\theta_2(\sin\theta_1 e^{i\phi_1}|E_1\rangle + \cos\theta_1 e^{i\phi_2}|E_2\rangle) \\ &\quad + \cos\theta_2|E_3\rangle \\ &\vdots \end{aligned} \quad (17)$$

where $0 \leq \theta_i \leq \frac{\pi}{2}$ and $0 \leq \phi_i \leq 2\pi$. It is observed that $2(n-1)$ parameters, $\theta_{1,2,\dots,n-1}$ and $\phi_{1,2,\dots,n-1}$, are required to determine an initial state up to a non-physical global phase.

We define the training set with N_{train} samples as

$$S = \{(X^1, Y^1), (X^2, Y^2), \dots, (X^{N_{train}}, Y^{N_{train}})\}. \quad (18)$$

In the k th sample, X^k is the input vector with $2(n-1)$ elements defined as

$$X^k = [\theta_1^k \ \theta_2^k \ \dots \ \theta_{(n-1)}^k \ \phi_1^k \ \phi_2^k \ \dots \ \phi_{(n-1)}^k]^T. \quad (19)$$

In this paper, we assume all the possible initial states are interested, thus θ_i^k and ϕ_i^k could be chosen as random numbers uniformly distributed in $[0, \frac{\pi}{2}]$ and $[0, 2\pi]$, respectively. For an initial state, the choice of its favorable control Hamiltonian is determined by simulating the dynamics with M candidate control Hamiltonians and

comparing the fidelities. The target output vector Y^k indicating the choices is a unit vector \vec{e} with $M + 1$ elements. For example, the control Hamiltonian could be mapped to the output vector Y by

$$\begin{aligned} H_1 &\longrightarrow \vec{e}_1 = [1 \ 0 \ \dots \ 0]^T, \\ H_2 &\longrightarrow \vec{e}_2 = [0 \ 1 \ \dots \ 0]^T, \\ &\vdots \\ H_M &\longrightarrow \vec{e}_M = [0 \ \dots \ 1 \ 0]^T, \\ \text{others} &\longrightarrow \vec{e}_{M+1} = [0 \ \dots \ 0 \ 1]^T, \end{aligned} \quad (20)$$

where *others* refer to cases without an optimal choice, e.g., ineffective controls or the existence of the same fidelities. On the other hand, a testing set S_T with N_{test} samples could be generated in a similar way as the training set eq.(18). The testing set (not participate in the supervised learning) is used for checking the performance of the neural network in order to avoid over training of the neural network.

Next, a feedforward neural network with $2(n-1)$ input nodes, $M + 1$ output neurons, plus some hidden layers is set up with the activation function Eq.(9). For an input vector X , the output of the neural network is a linear combination of all the basis vectors, i.e.,

$$Y' = \sum_{j=1}^{M+1} q_j \vec{e}_j, \quad 0 < q_j < 1. \quad (21)$$

The classification is implemented by selecting the choice with the largest coefficient q_j . Here q_j might be understood as an unnormalized probability that the choice is j . The performance of a neural network could be measured by the mean squared error (MSE)

$$MSE = \frac{1}{N} \sum_{k=1}^N (Y'^k - Y^k)^T (Y'^k - Y^k) \quad (22)$$

where Y'^k is the output of the neural network for X^k and Y^k is the k th target output vector. N is the number of the training (or testing) samples.

With the training set Eq.(18) determined by Eq.(19) and Eq.(20), the weights and biases could be effectively trained by the back propagation (BP) algorithm. The iteration number of the BP training process could be determined by checking the mean squared error (or the classification success rate) for the testing set. Before the training (testing) process, the input vector $X^k = [x_1^k \ x_2^k \ \dots \ x_{n_I}^k]$ is normalized to $X'^k = [x_1'^k \ x_2'^k \ \dots \ x_{n_I}'^k]$ by $x_j'^k = 2(x_j^k - x_j^{min}) / (x_j^{max} - x_j^{min}) - 1$ where x_j^{max} (x_j^{min}) is the maximum (minimum) of the N_{train} input vector elements x_j^k ($k = 1, 2, \dots, N_{train}$) from the training set. In this way, all the signals sent to the input nodes are scaled to the range $[-1, 1]$ in order to be sensitive to the sigmoid functions of the neural network. Finally, the trained neural network will be used to select control

Hamiltonian for new initial states (out of the training set). For the problem of selecting other control schemes, our method may also be applied in a similar way.

B. Regression: designing Lyapunov function

In this section, GRNN is used to design an initial-state-adaptive Lyapunov function V of the form Eq.(2) where $P = f_{GRNN}(|\Psi_0\rangle)$. The system Hamiltonian H_0 and control Hamiltonian(s) H_k are fixed. The task is to prepare an eigenstate of H_0 with a high fidelity defined as $F = |\langle \Psi(T) | E_g \rangle|^2$ at time T .

Notice that the strength coefficient K in Eq.(6) can be absorbed into the operator P , i.e., $V' = \langle \psi | K P | \psi \rangle = \langle \psi | P' | \psi \rangle$. Therefore, we set $K = 1$ and merely discuss P for simplicity. Assume the goal state is the g th eigenstate of H_0 denoted by $|E_g\rangle$. For a n -dimensional system, the operator P is designed as

$$\begin{aligned} P &= p_g |E_g\rangle \langle E_g| + \sum_{l \neq g} p_l |E_l\rangle \langle E_l| \\ &= \sum_{l \neq g} p_l |E_l\rangle \langle E_l| \quad (p_l > p_g = 0). \end{aligned} \quad (23)$$

We have set the minimum coefficient p_g to 0 without loss of generality, since if $p_g \neq 0$, one can shift it to zero by adding $-p_g \sum_l |E_l\rangle \langle E_l| = -p_g I$ to P , which does not change the control fields according to Eq.(6). Now the favorable Lyapunov function for an initial state could be obtained by optimizing $p_{l(l \neq g)}$ numerically. The number of p_l to be optimized is $n - 1$. In principle, there are no limitation on the bound of p_l in optimization. However, some constraints of p_l are required to limit the strength of the control fields and facilitate the numerical optimizations, e.g., $0 < p_l \leq p_l^{max}$.

In this method, the training set (testing set if needed) with N_{train} (N_{test}) samples can be defined similarly as Eq.(18). The input vector X^k is given by Eq.(19) and the k th output vector Y^k is defined as

$$Y^k = [p_1^k \ p_2^k \ \dots \ p_{n-1}^k]^T. \quad (24)$$

The elements of the target vector $p_{j=1,2,\dots,n-1}^k$ are the optimal values in one-to-one correspondence with p_l in Eq.(23). Given an input vector X^k (an initial state), Y^k is obtained by numerically finding p_j^k that maximizing the fidelity F_k with the constraints of p_j^k , in which the dynamics needs to be simulated many times.

With the training set, a GRNN with $2(n-1)$ input nodes, N_{train} pattern layer neurons and $n-1$ output neurons can be built straightforwardly. The smoothing parameter σ (defined in Eq.(13)) could be determined by checking the GRNN performance for the testing samples without many trials. Different performances for the testing samples might be used such as the MSE or the

averaged logarithmic infidelity defined by

$$\epsilon = \frac{1}{N} \sum_{k=1}^N \log(1 - F_k). \quad (25)$$

Since the smoothing parameter σ (connected with the width of the Gaussian function in Eq.(13)) is the same for all the input vector elements, the input vectors need to be normalized such that σ is sensitive to all the input vector elements. Let each input vector element be normalized to $[-1, 1]$ as in the last design, then the average space between two neighboring (normalized) input vectors could be estimated by $D = 2/\sqrt[n]{N_{train}}$ where $n_I = 2(n-1)$ is the dimension of the input vector. We suggest to find the smoothing parameter in the range $0 < \sigma < \sigma_{max}$ where $\sigma_{max} \sim D$. With an appropriate σ , the GRNN will be finally used to predict optimal P of the Lyapunov function for new initial states.

V. ILLUSTRATION

In this section, we illustrate our designs with a three-level quantum system ($n=3$). The time-independent system Hamiltonian is described by

$$H_0 = \sum_{n=1}^3 \omega_n |n\rangle\langle n| + g(|1\rangle\langle 2| + |2\rangle\langle 1|), \quad (26)$$

where ω_n is the frequency of the n th level and the state $|2\rangle$ and $|1\rangle$ are coupled with a strength g . The task is to prepare an eigenstate of H_0 with high fidelity, e.g., $|E_3\rangle$ where E_3 is the highest eigenenergy. The fidelity is calculated by $F = |\langle \Psi(T) | E_3 \rangle|^2$ with T the control time. The dynamics is described by Eq.(16) and the control field is given by Eq.(6).

A. Selecting control Hamiltonians

To illustrate the first design, consider two candidate control Hamiltonians ($M = 2$),

$$H_1 = |1\rangle\langle 3| + |3\rangle\langle 1|, \quad (27)$$

$$H_2 = |2\rangle\langle 3| + |3\rangle\langle 2|. \quad (28)$$

Given an arbitrary initial state $|\Psi_0\rangle$, we will use a feedforward neural network to select the control Hamiltonian that leads to a higher fidelity. In this example, $P = |E_1\rangle\langle E_1| + |E_2\rangle\langle E_2| = I - |E_3\rangle\langle E_3|$ is used in the Lyapunov function of the form Eq.(2). Thus $V = \langle \Psi | P | \psi \rangle = 1 - |\langle \Psi | E_3 \rangle|^2$ might be understood as either Eq.(23) with $p_1 = p_2 = 1$ (unoptimized) or a distance between the controlled state and the goal state. According to our method, the input vectors in the training (testing) set are given by $X^k = [\theta_1^k \ \theta_2^k \ \phi_1^k \ \phi_2^k]^T$, $k = 1, 2, \dots, N_{train}(N_{test})$ where $\theta_{1,2}^k$ and $\phi_{1,2}^k$ is defined as in Eq.(17) with $n = 3$.

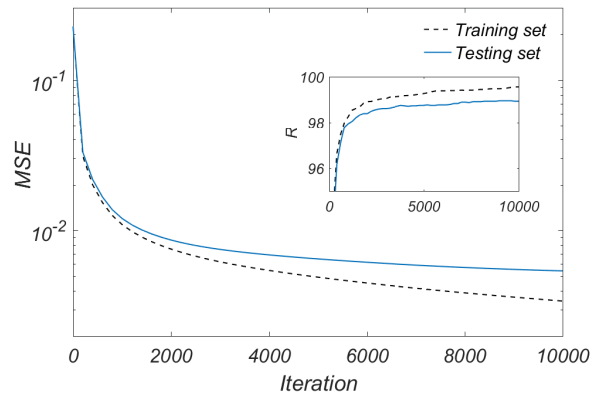


FIG. 3: The training process of the feedforward neural network. Mean figure: the Mean squared error (MSE) for the training set (black dashed line) and the testing set (blue solid line) versus the iteration number. Inset: the percentage of the classification success rate (R) for the training set and the testing set.

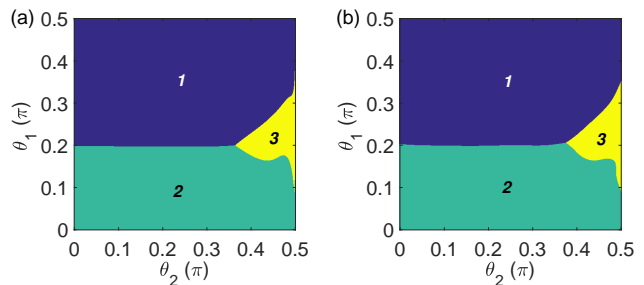


FIG. 4: The dependence of the control Hamiltonian choices on θ_1 and θ_2 with $\phi_1 = \phi_2 = 0$ (blue for H_1 , green for H_2 and yellow for low or the same fidelities). Results in (a) are calculated by simulating the dynamics with H_1 and H_2 and results in (b) are predicted by the neural network. Each subfigure contains 500×500 pixels corresponding to different θ_1 and θ_2 .

We consider 3 choices (H_1 , H_2 and *others*) corresponding to target output vectors $\vec{e}_{1,2,3}$, respectively. Here the *others* refers to the same fidelities or both fidelities less than 0.99.

For illustrating the training process, we generated a training set with 10^4 samples (59% H_1 , 37% H_2 and 4% low or the same fidelities) plus a testing set with $N_{test} = 5 \times 10^3$ samples through simulating the dynamics. In our simulations, the control parameters are $\omega_2 = 2\omega_1$, $\omega_3 = 5\omega_1$, $g = 0.5\omega_1$, $K = 1$, and the control time is $T = 20/\omega_1$. We set up a feedforward neural network with 4 input nodes, 3 output neurons and 2 hidden layers of 30 neurons, respectively. The feedforward neural network was trained by a back propagation algorithm to minimize the MSE for the training set where a gradient descent method with momentum and adaptive learning rate was used. The training process is illustrated in Fig.3 where the MSEs and the classification success rates R

for the training set and the testing set are plotted (with 10^4 iterations). The MSEs for both set decreased dramatically in the first thousand iterations together with a rapid increase of the classification success rates (exceed 97%). The training set MSE monotonically decrease through the training process due to the gradient algorithm, whereas the testing set MSE might slightly oscillate in the later iterations.

TABLE I: Feedforward neural network performances for different numbers of training samples

N_{train}	N_{test}	MSE (Testing)	Iteration	R_A
1×10^1	5×10^3	0.1060	1.5×10^3	78.3%
1×10^2	5×10^3	0.0490	3.5×10^4	90.5%
1×10^3	5×10^3	0.0171	2.4×10^3	96.8%
1×10^4	5×10^3	0.0051	1.92×10^4	98.7%
4×10^4	5×10^3	0.0034	1×10^5	99.3%

We then conducted 5 studies with different numbers of training samples N_{train} where the testing sample numbers $N_{test} = 5 \times 10^3$ are the same for comparison. The control parameters and the neural network structure are the same as those in Fig.3. In these studies, we adopted the iteration numbers corresponding to the minimal testing set MSEs (in at most 1×10^5 iterations) to determine the weights and biases of the neural networks. Finally, the trained neural networks were applied to predict control Hamiltonians for 5×10^4 new random initial states as applications. The corresponding classification success rates, denoted by R_A , and other training details are shown in Table.I. It is seen that the success rate R_A was greater than 90% even with 100 training samples in this example. In these studies, the MSEs for the testing set almost decreased to their minimums with thousands of iterations. We then checked the dependence of the control Hamiltonian choice on θ_1 and θ_2 ($\phi_1 = \phi_2 = 0$ is set) predicted by the neural network trained with 4×10^4 samples. The result is similar to the real result (calculated by simulating the dynamics) as shown in Fig.4. The processing time of the feedforward neural network depends on its layer number and node number in each layer. For Fig.4, the processing time of the feedforward neural network for Fig.4(b) was typically 1.5-5.5 orders lower than the simulation time for Fig.4(a) on our computer, depending on how the input vectors were sent to the neural network function, one-by-one or in batch.

B. Designing Lyapunov functions

In the second illustration, we will use GRNN to design initial-state-adaptive Lyapunov functions where one control Hamiltonian H_1 given by Eq.(27) is used. The control parameters are $\omega_2 = 2\omega_1$, $\omega_3 = 5\omega_1$, $g = 0.5\omega_1$, $K = 1$ and $T = 2\pi/\omega_1$. The operator P is designed by $P = p_1|E_1\rangle\langle E_1| + p_2|E_2\rangle\langle E_2|$ ($p_3 = 0$) according to Eq.(23).

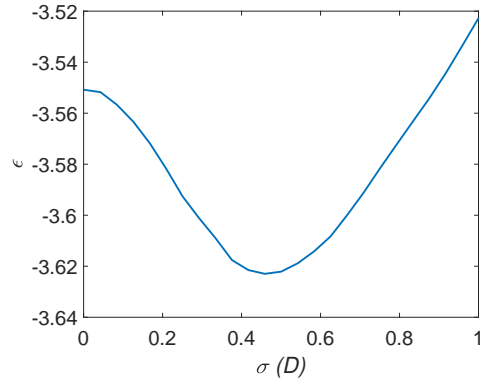


FIG. 5: The dependence of the averaged logarithmic infidelity ϵ for 2×10^3 testing samples on the smoothing parameter σ (defined in Eq.(13)) of the GRNN.

We generated totally 10^5 samples for training where the input vector is $X^k = [\theta_1^k \theta_2^k \phi_1^k \phi_2^k]^T$ and the target output vector is $Y^k = [p_1^k p_2^k]^T$. Here p_1^k and p_2^k correspond to p_1 and p_2 , respectively, which were found by minimizing the infidelity with the interior-point algorithm using the MATLAB optimization toolbox. For each random initial state, 8 optimizations with different (random) starting points were implemented to avoid local minimums. $p_{1,2}$ were optimized with the constraints $0 \leq p_1 \leq 10, 0 \leq p_2 \leq 20$. It is observed that the optimal values of $p_{1,2}$ corresponding to over 96% of the initial states lie inside the area given by the constraints (rather than near the edges of the area), implying the constraints are plausible. The averaged logarithmic infidelity ϵ (defined by Eq.(25)) for these training samples is -4.03 and the fraction of fidelities that are greater than 0.999 is $R_{F>0.999} = 0.773$.

With a training set of $N_{train} = 5 \times 10^4$ samples, we set up a GRNN with 4 input nodes, 2 output neurons, 3 summation layer neurons and N_{train} pattern layer neurons. The smoothing parameter σ was determined by checking the averaged logarithmic infidelity ϵ for $N_{test} = 2 \times 10^3$ random initial states (out of the training set) with several trials and choosing the smoothing parameter with the minimal ϵ . The dependence of ϵ on the smoothing parameter σ is shown in Fig.5 with $0.001D \leq \sigma \leq D$ where $D = 2/\sqrt[4]{N_{train}}$ is the average space between two neighboring normalized input vectors introduced in Sec.IV B. Finally, $\sigma = 0.46D$ was adopted for the GRNN. As an application, the trained GRNN was used to predict Lyapunov functions for $N_{app} = 10^5$ new (random) initial states. The averaged logarithmic infidelity and the fraction of $F > 0.999$ is $\epsilon = -3.61$ and $R_{F>0.999} = 0.715$, respectively. To further demonstrate the performance of the GRNN, we plot the distribution of the infidelities of the application procedure in Fig.6. This distribution is compared with that of the 10^5 training samples and that from an initial-state-independent Lyapunov control with $P_{ind} = 0.759|E_1\rangle\langle E_1| + 3.683|E_2\rangle\langle E_2|$ for $N_{app} = 10^5$ ran-

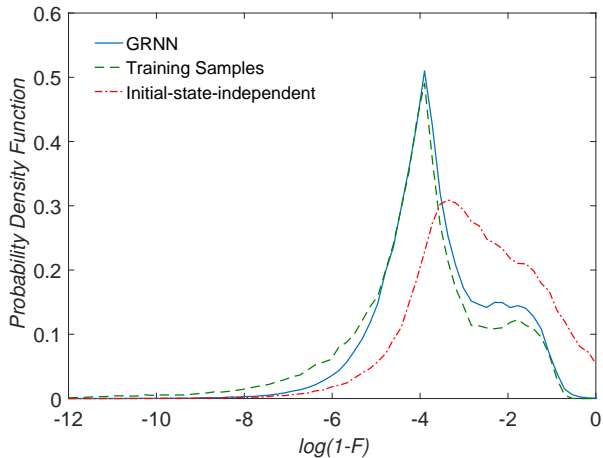


FIG. 6: Infidelity distributions for 10^5 random initial states with different control schemes. The blue (solid) line and green (dashed) line represent the distribution from the GRNN control and that of the training samples (by numerical optimizations), respectively. The red (dot-dashed) line represents the result with an initial-state-independent (optimized) Lyapunov function.

dom initial states (see Fig.6). Here P_{ind} was obtained by a numerical optimization that minimized the averaged logarithmic infidelity for 2×10^3 testing random initial states. The infidelity distribution from the GRNN-designed control is similar to that of the training samples, both with a peak at about $\log(1 - F) = -4$, while the probability density functions with $\log(1 - F) < -5$ and $-3 < \log(1 - F) < -1$ are slightly different. In contrast, the initial-state-independent control generated more low-fidelity states with an averaged logarithmic infidelity $\epsilon = -2.76$ and $R_{F>0.999} = 0.443$, although P_{ind} had been optimized. We remind that an arbitrary unoptimized initial-state-independent P leads to a much worse result. For example, $p_1 = p_2 = 10$ lead to $\epsilon = -1.26$ and $R_{F>0.999} = 0.048$ in a simulation with $N_{app} = 10^5$ random initial states.

TABLE II: GRNN performances for different numbers of training samples

N_{train}	σ	ϵ	$R_{F>0.999}$	$R_{F>0.999}(train)$
5×10^3	$0.50D$	-3.41	0.657	0.773
1×10^4	$0.50D$	-3.47	0.678	0.773
5×10^4	$0.50D$	-3.60	0.716	0.773
1×10^5	$0.50D$	-3.64	0.722	0.773

In this example, we found empirically that the optimal smoothing parameters are generally near $0.5D$ either use ϵ or the MSE as the performance measure, regardless of the training sample number. The reason is that the distribution of the (normalized) training input vectors in the GRNN is known (with an average space D) and when $\sigma = 0.5D$, the full width at half maximum of the Gaussian function in Eq.(13) is roughly D . Such a Gaus-

sian function probably leads to a good performance of a GRNN which could be understood by examining curve fitting problems. Thus one might find optimal σ near $0.5D$ or use $0.5D$ for simplicity.

We further tested the performances of several GRNNs based on different numbers of training samples with $\sigma = 0.5D$. The GRNNs were applied to the same Lyapunov control problem for $N_{app} = 10^5$ random initial states. The details are shown in Table II. As the number of training samples increases, the performance of the GRNN became better, together with a longer processing time of the GRNN due to its increased size. In our study, the longest prediction time (for one initial state) of the GRNN based on 10^5 training samples was roughly the time of simulating the dynamics once. Meanwhile, finding an optimal P in our numerical optimizations (with 8 starting points) typically required simulating the dynamics about 6 hundred times. Thus, the initial-state-adaptive control with GRNN is able to improve the control performance with significantly less computing resources compared with that by numerical optimizations.

VI. SUMMARY AND DISCUSSION

We have proposed two initial-state-adaptive Lyapunov control designs with machine learning where the feedforward neural network and the GRNN are used to select control schemes and predict Lyapunov functions for different initial states. The aim of the designs is to improve the control performance for different initial states without much increase of computing resources. Our methods could be applied to Lyapunov control problems when many initial states are involved or real-time processing is needed. The neural networks are trained by samples which are numerically generated before the final applications. We illustrated our designs with a three-level eigenstate control problem. Our results show that the neural networks are able to effectively learn the relationship between the initial states and the optimal control schemes or optimal Lyapunov functions and make predictions. The processing time of the neural networks are significantly less than that by numerical methods in our examples.

In our examples, the samples were divided into one training set and one testing set where we have assumed that the number of testing samples is large enough to reflect the generalization ability of the neural networks. When the number of samples is limited, other methods such as a k-fold cross validation [24] might be used to fully take advantage of the samples. In our examples, the raw training data generated from simulations were used for the GRNN. In fact, our investigations showed that some simple processing of the raw training data may further improve the GRNN performance, for example, modestly removing the samples near the edge of the search area (given by $0 < p_l \leq p_l^{max}$). The reason is that the relation between the optimal parameters and

initial states may become less noisy after the data processing, although the training sample number is reduced. In general, the number of training samples and the size of neural networks significantly increase with the system dimension, the problem might be circumvented by investigating the initial-state-adaptive control with a subspace of all the possible initial states. Our initial-state-adaptive Lyapunov designs might also be used for other Lyapunov control problems to classify the initial states or predict continues parameters, such as the operator in Lyapunov function and the control fidelity.

VII. ACKNOWLEDGMENTS

This work is supported by the National Natural Science Foundation of China under Grant No. 11705026, 11534002, 11775048, 61475033, the China Postdoctoral Science Foundation under Grant No. 2017M611293, and the Fundamental Research Funds for the Central Universities under Grant No. 2412017QD003.

-
- [1] D'Alessandro, D. *Introduction to Quantum Control and Dynamics* (Taylor and Francis Group, Boca Raton London New York, 2007).
- [2] Wiseman, H. M., and Milburn, G. J. *Quantum Measurement and Control* (Cambridge University Press, Cambridge, England, 2009).
- [3] Vettori, P. (2002). On the convergence of a feedback control strategy for multilevel quantum systems. In Proceedings of the MTNS Conference (pp. 1-6).
- [4] Grivopoulos, S., and Bamieh, B. (2003, December). Lyapunov-based control of quantum systems. In Decision and Control, 2003. Proceedings. 42nd IEEE Conference on (Vol. 1, pp. 434-438). IEEE.
- [5] Mirrahimi, M., Rouchon, P., and Turinici, G. (2005). Lyapunov control of bilinear Schrödinger equations. *Automatica*, 41(11), 1987-1994.
- [6] Kuang, S., and Cong, S. (2008). Lyapunov control methods of closed quantum systems. *Automatica*, 44(1), 98-108.
- [7] Wang, X., and Schirmer, S. G. (2010). Analysis of Lyapunov method for control of quantum states. *IEEE Transactions on Automatic control*, 55(10), 2259-2270.
- [8] Hou, S. C., Khan, M. A., Yi, X. X., Dong, D., and Petersen, I. R. (2012). Optimal Lyapunov-based quantum control for quantum systems. *Physical Review A*, 86(2), 022321.
- [9] Wang, L. C., Hou, S. C., Yi, X. X., Dong, D., and Petersen, I. R. (2014). Optimal Lyapunov quantum control of two-level systems: Convergence and extended techniques. *Physics Letters A*, 378(16-17), 1074-1080.
- [10] Zhao, S., Lin, H., and Xue, Z. (2012). Switching control of closed quantum systems via the Lyapunov method. *Automatica*, 48(8), 1833-1838.
- [11] Kuang, S., Dong, D., and Petersen, I. R. (2017). Rapid Lyapunov control of finite-dimensional quantum systems. *Automatica*, 81, 164-175.
- [12] Silveira, H. B., da Silva, P. P., and Rouchon, P. (2016). Quantum gate generation for systems with drift in $U(n)$ using Lyapunov/CLaSalle techniques. *International Journal of Control*, 89(12), 2466-2481.
- [13] Wang, X. and Schirmer, S. G. (2009). Entanglement generation between distant atoms by Lyapunov control. *Physical Review A*, 80(4), 042305.
- [14] Yi, X. X., Huang, X. L., Wu, C., and Oh, C. H. (2009). Driving quantum systems into decoherence-free subspaces by Lyapunov control. *Physical Review A*, 80(5), 052316.
- [15] Sayrin, C., Dotsenko, I., Zhou, X., Peaudecerf, B., Rybarczyk, T., Gleyzes, S., ... and Raimond, J. M. (2011). Real-time quantum feedback prepares and stabilizes photon number states. *Nature*, 477(7362), 73.
- [16] Dong, D., and Petersen, I. R. (2012). Sliding mode control of two-level quantum systems. *Automatica*, 48(5), 725-735.
- [17] Hou, S. C., Wang, L. C., and Yi, X. X. (2014). Realization of quantum gates by Lyapunov control. *Physics Letters A*, 378(9), 699-704.
- [18] Shi, Z. C., Zhao, X. L., and Yi, X. X. (2015). Robust state transfer with high fidelity in spin-1/2 chains by Lyapunov control. *Physical Review A*, 91(3), 032301.
- [19] Shi, Z. C., Zhao, X. L., and Yi, X. X. (2015). Preparation of topological modes by Lyapunov control. *Scientific reports*, 5, 13777.
- [20] Shi, Z. C., Hou, S. C., Wang, L. C., and Yi, X. X. (2016). Preparation of edge states by shaking boundaries. *Annals of Physics*, 373, 286-297.
- [21] Li, W., Li, C., and Song, H. (2016). Quantum synchronization in an optomechanical system based on Lyapunov control. *Physical Review E*, 93(6), 062221.
- [22] Ran, D., Shi, Z. C., Song, J., and Xia, Y. (2017). Speeding up adiabatic passage by adding Lyapunov control. *Physical Review A*, 96(3), 033803.
- [23] Li, C., Song, J., Xia, Y., and Ding, W. (2018). Driving many distant atoms into high-fidelity steady state entanglement via Lyapunov control. *Optics Express*, 26(2), 951-962.
- [24] Alpaydin, E. *Introduction to machine learning* (MIT Press, Cambridge Massachusetts, 2010) 2nd ed.
- [25] Haykin, S. S. *Neural networks and learning machines* (Pearson, New Jersey, 2009) 3rd ed.
- [26] Magesan, E., Gambetta, J. M., Crocoles, A. D., and Chow, J. M. (2015). Machine learning for discriminating quantum measurement trajectories and improving readout. *Physical review letters*, 114(20), 200501.
- [27] Mills, K., Spanner, M., and Tamblyn, I. (2017). Deep learning and the Schrödinger equation. *Physical Review A*, 96(4), 042113.
- [28] Melnikov, A. A., Nautrup, H. P., Krenn, M., Dunjko, V., Tiersch, M., Zeilinger, A., and Briegel, H. J. (2018). Active learning machine learns to create new quantum experiments. *Proceedings of the National Academy of Sciences*, 201714936.
- [29] Torlai, G., Mazzola, G., Carrasquilla, J., Troyer, M., Melko, R., and Carleo, G. (2018). Neural-network quan-

- tum state tomography. *Nature Physics*, 14(5), 447.
- [30] Carleo, G., and Troyer, M. (2017). Solving the quantum many-body problem with artificial neural networks. *Science*, 355(6325), 602-606.
- [31] Deng, D. L. (2018). Machine Learning Detection of Bell Nonlocality in Quantum Many-Body Systems. *Physical Review Letters*, 120(24), 240402.
- [32] Gao, J., Qiao, L. F., Jiao, Z. Q., Ma, Y. C., Hu, C. Q., Ren, R. J., ... and Jin, X. M. (2018). Experimental Machine Learning of Quantum States. *Physical Review Letters*, 120(24), 240501.
- [33] Zahedinejad, E., Ghosh, J., and Sanders, B. C. (2016). Designing high-fidelity single-shot three-qubit gates: a machine-learning approach. *Physical Review Applied*, 6(5), 054005.
- [34] Mavadia, S., Frey, V., Sastrawan, J., Dona, S., and Biercuk, M. J. (2017). Prediction and real-time compensation of qubit decoherence via machine learning. *Nature communications*, 8, 14106.
- [35] August, M., and Ni, X. (2017). Using recurrent neural networks to optimize dynamical decoupling for quantum memory. *Physical Review A*, 95(1), 012335.
- [36] Yang, X. C., Yung, M. H., and Wang, X. (2018). Neural-network-designed pulse sequences for robust control of singlet-triplet qubits. *Physical Review A*, 97(4), 042324.
- [37] Specht, D. F. (1991). A general regression neural network. *IEEE transactions on neural networks*, 2(6), 568-576.
- [38] Leung, M. T., Chen, A. S., and Daouk, H. (2000). Forecasting exchange rates using general regression neural networks. *Computers & Operations Research*, 27(11-12), 1093-1110.
- [39] Li, C., Bovik, A. C., and Wu, X. (2011). Blind image quality assessment using a general regression neural network. *IEEE Transactions on Neural Networks*, 22(5), 793-799.
- [40] Liu, J., Bao, W., Shi, L., Zuo, B., and Gao, W. (2014). General regression neural network for prediction of sound absorption coefficients of sandwich structure nonwoven absorbers. *Applied Acoustics*, 76, 128-137.
- [41] Panda, B. N., Bahubalendruni, M. R., and Biswal, B. B. (2015). A general regression neural network approach for the evaluation of compressive strength of FDM prototypes. *Neural Computing and Applications*, 26(5), 1129-1136.